An Exploration of the CEV Process

John Lee

December 15, 2023

Abstract

This paper provides a comprehensive exploration of the Constant Elasticity of Variance (CEV) process, a stochastic differential process integral to financial mathematics. It delves into the historical development of the process, highlighting its role in option pricing and its advancements over the traditional Black-Scholes model. Central to this study is the 'constant of elasticity' term, α, which characterizes the relationship between the underlying asset price and volatility within the CEV process, offering a more realistic depiction of market dynamics. The paper investigates the mathematical underpinnings of the CEV process, particularly focusing on the transition density function and its norm-decreasing property within the $\alpha < 1$ regime. Additionally, the research employs an Euler-Maruyama (EM) scheme and a direct sampling scheme to simulate the CEV process for various option strike prices ($K = 90, 100, 110$), comparing simulated call and put option prices to analytically computed values for different values of the elasticity parameter, alpha. Additionally, due to high error measurements, an analysis of discretization errors in the EM scheme for negative values of the elasticity parameter is performed. This research provides valuable insights into the applicability, theoretical, and computational aspects of the CEV process.

1 Introduction

Options, as financial instruments, grant the holder the right, but not the obligation, to buy or sell an underlying asset at a predetermined price within a specified time frame. This definition encapsulates two primary types of options: calls, which provide the right to purchase, and puts, which offer the right to sell. In the realm of financial mathematics, options have become a fundamental instrument, providing investors with the flexibility to hedge risks or speculate on future market movements. The concept of options dates back to ancient times, but the modern framework for options pricing emerged in the 20th century, coinciding with the development of sophisticated financial markets. The Chicago Board Options Exchange (CBOE) was established in 1973, marking the first organized options exchange, which greatly increased the accessibility and standardization of options trading.

With the onset of mass options trading, research in options pricing schemes began skyrocketing. IN 1973, the landmark Black-Scholes model, publicly introduced by Fischer Black and Myron Scholes, revolutionized the field by providing a systematic approach to pricing

European-style options [1]. This model, which assumes constant volatility and a log-normal distribution of stock prices, has been celebrated for its simplicity and mathematical elegance, and it laid the foundation for the contemporary options market. Despite its groundbreaking impact, the Black-Scholes model has notable limitations, primarily the assumption of constant volatility. This limitation was made evident in the market crash of 1987 and has since been widely criticized, as empirical studies show that market volatility is stochastic and varies over time [6]. These limitations spurred further research into alternative models that could more accurately capture market behaviors.

One such development is the Constant Elasticity of Variance (CEV) process, introduced by John Cox in 1975. The CEV model addresses a critical limitation of the Black-Scholes model by allowing the volatility of the underlying asset to be a function of the asset price itself, thereby introducing a 'smile' effect in implied volatility that is observed in real markets [2]. The CEV model's flexibility in modeling volatility dynamics makes it a valuable tool for pricing options in markets exhibiting stochastic or patterned volatility, offering a more nuanced and realistic approach compared to the Black-Scholes model.

In this study, I explore several mathematical properties and provide simulations of the CEV process. The paper is organized as follows. First, in Section 2, I introduce the mathematics of the CEV process, discussing its relationship to the Black Scholes model and other mathematical properties. Then, in Section 3, methodology and simulations of the CEV process through the Euler-Maruyama discretization scheme are presented, with comparisons to analytical values. I take a closer look at the discretization scheme for negative values of α in Section 3.5, and lastly, some conclusions and future work are discussed in Section 4.

2 Mathematics of the CEV Process

2.1 Black Scholes Model

The Black-Scholes Model described in [1] is primarily recognized as a partial differential equation with an analytical form determining the price of a European call option at expiry. However, the Black-Scholes Model can also be understood as a stochastic process, the underlying stochastic differential equation a direct application of Geometric Brownian Motion,

$$dF = \mu dt + \sigma_{LN} F dW \quad F(0) = F_0 > 0 \tag{1}$$

where F is the price of an underlying asset, μ is a drift term, σ is the annual lognormal volatility of a stock, and dW is a Weiner process. The stochastic differential equation is defined up to a time T in years. The volatility term, σ_{LN}, remains constant throughout the entire period, confirming the constant volatility assumption.

2.2 SDE of the CEV Model

The CEV process is a time-diffusion process containing a conceptually simple extension of geometric Brownian motion,

$$df = \mu dt + \sigma F^{\alpha} dW, \quad F(0) = F_0 > 0 \tag{2}$$

where α is an additional parameter known as the constant of elasticity. In order to maintain the dimensionality of σ, we let

$$\sigma = \sigma_{LN} F^{1-\alpha} \tag{3}$$

be the instantaneous value of volatility.

Now, depending on the value for the constant of elasticity, α, three unique regimes can be identified within the CEV process as shown via the Fokker-Plank equations by Feller in [3]. These regimes can be interpreted from both a financial or mathematical perspective as follows

1. $\alpha > 1$. In this regime, σ is inversely related to price and leverage ratios increase, a commonly observed occurrence in equity markets. This relationship is rigorously explored in [9].

2. $0.5 < \alpha < 1$. In this regime, σ is positively related to price, a common occurrence in commodity markets [4]. Additionally, a boundary of $F = 0$ is attainable and absorbing. This absorption results in interesting mathematical behavior discussed in Section 2.4

3. $\alpha < 0.5$. This regime also results in a positive correlation between volatility and price. The boundary $F = 0$ is attainable and can be either reflecting or absorbing.

4. $\alpha = 1$. While not a regime, this case mathematically evaluates back to the original Black-Scholes diffusion process.

2.3 X-Transform

For the rest of this paper, we focus our exploration by eliminating the drift term, $\mu = 0$, and address only the mathematics of the $\alpha < 1$ case. We choose $F = 0$ to be an absorbing boundary condition for all α.

$$dF = \sigma F^{\alpha} dW \quad F(0) = F_0 > 0, \alpha < 1 \tag{4}$$

When observing the CEV process, as mentioned in [7], it is significantly advantageous to deal with the transformed variable, X, and its corresponding stochastic differential equation

$$X = \frac{F^{2(1-\alpha)}}{\sigma^2(1-\alpha)^2}, \quad dX = \delta dt + \sigma\sqrt{X} dW, \quad \delta = \frac{1-2\alpha}{1-\alpha} \tag{5}$$

The SDE in equation 5 is easily verified by Ito's lemma (see Appendix A) and is known as the squared Bessel process with δ degrees of freedom.

For positive integer δ, the Bessel process governs the squared distance, X, from the origin of a Brownian particle in δ spatial dimensions, and is known to have a non-central chi-squared distribution

$$\rho_{\chi'^2}(x; \delta, \lambda) = \frac{1}{2}\left(\frac{x}{\lambda}\right)^{\nu/2} \exp\left[-\frac{x+\lambda}{2}\right] I_\nu(\sqrt{x\lambda}), \quad \nu = \frac{\delta}{2} - 1 \tag{6}$$

where $\chi'^2(x; k, \lambda)$ is the non-central chi-squared distribution with k degrees of freedom and non-centrality parameter λ, and I_ν is the modified Bessel function of the first kind with index ν [7]. In the CEV process, δ may not necessarily be a positive integer (as it depends on α), but this relationship is important for the next section.

2.4 Transition Density Function

By solving the Fokker-Plank equations using Laplace Transforms on the squared Bessel process in equation 5, the transition density function

$$\rho_\delta(X_T, T; X_0) = \frac{1}{2T}(\frac{X_T}{X_0})^{\nu/2} \exp\left[-\frac{X_T + X_0}{2T}\right] I_{-\nu}\left(\frac{\sqrt{X_T X_0}}{T}\right) \tag{7}$$

can be found. Refer to [5] for a detailed derivation. In [7], it is noted that an inspection of the TDF reveals a relation to the non-central chi-squared distribution as follows,

$$\rho_\delta(X, T; X_0) = \rho_{\chi'^2}\left(\frac{X_0}{T}; 4 - \delta, \frac{X}{T}\right)\frac{1}{T}. \tag{8}$$

The $F = 0$ absorbing boundary mentioned in Section 2.2 is preserved as $X = 0$ in the transformation to X. Due to the absorbing nature of the $X = 0$ boundary, it is possible to lose probability mass. In [7], a direct integration of $\rho_\delta(X, T; X_0)$ is taken, finding

$$\int_0^\infty \rho_\delta(X, T; X_0)dX = \Gamma\left(-\nu; \frac{X_0}{2T}\right) \leq 1 \tag{9}$$

where Γ is the normalized incomplete gamma function

$$\Gamma(n; x) = \frac{1}{\Gamma(n)}\int_0^x t^{n-1}e^{-t}dt. \tag{10}$$

Cases of equation 9 with strictly less than one are known as norm-*decreasing*, while cases of equality to one are known as norm-*preserving*. In our simulations in Section 3, we can verify the absorption ratio using this relationship.

Since ρ_δ is norm-decreasing, the full TDF is the sum of ρ_δ and a Dirac measure at zero,

$$\rho_\delta^{\text{full}}(X_T, T; X_0) = 2\left[1 - \Gamma\left(-\nu; \frac{X_0}{2T}\right)\right]\delta(X_T) + \rho_\delta(X, T; X_0). \tag{11}$$

Combining equation 8 and 11, we find that X is distributed according to

$$Pr(X \leq X_T | X_0) = \int_0^{X_T} \rho_\delta^{\text{full}}(X_T, T; X_0)dX = 1 - \chi'^2(X_0; 2 - \delta; x) \tag{12}$$

2.5 Analytical Options Pricing Formula

From the CEV process, an analytical options pricing formula can be established just like the Black-Scholes equation. For a European at-expiry option, its value can be determined by the equation

$$C = E[\max(F_T - K, 0)|F_0] = \int_K^\infty (F - K)\rho_\delta(F, T; F_0)dF, \tag{13}$$

where F_T is the final price of the underlying, K is the strike price, and T is the expiration date. According to [8], the integral in equation 13 can be computed in the $\alpha < 1$ regime as

$$C_{\alpha<1} = F_0 \left[1 - \chi'^2\left(\frac{\tilde{K}}{T}; 4-\delta, \frac{X_0}{T}\right)\right] - K\chi'^2\left(\frac{X_0}{T}; 2-\delta, \frac{\tilde{K}}{T}\right), \quad \tilde{K} = \frac{K^{2(1-\alpha)}}{\sigma^2(1-\alpha)^2} \tag{14}$$

providing an analytical solution for European call options. Additionally, we can find the equivalent put option prices through put-call parity:

$$P_{\alpha<1} = C_{\alpha<1} - F_0 + K. \tag{15}$$

3 Simulations of the CEV Process

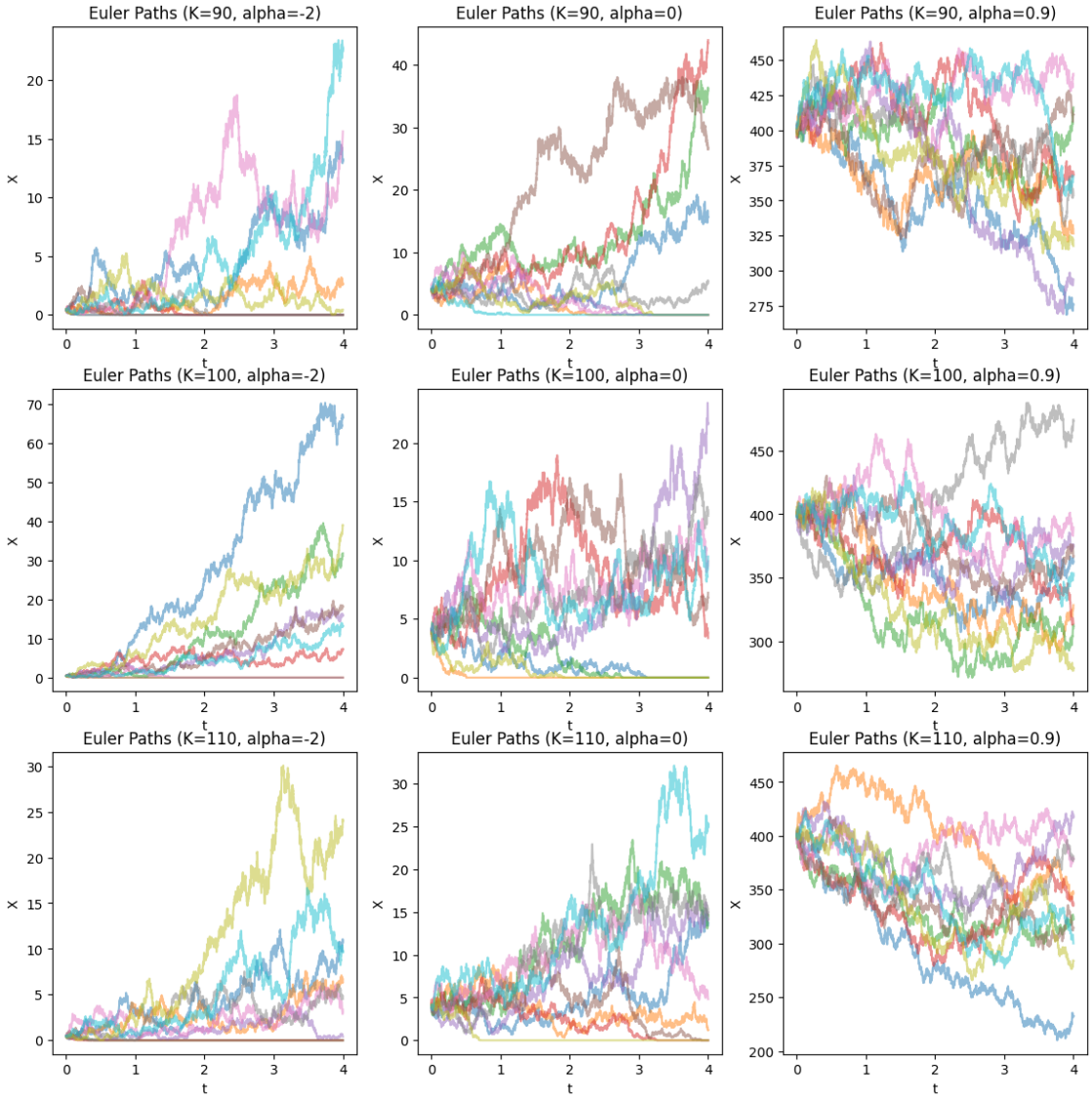

Figure 1: Euler path simulations of X for K = 90,100,110 and alpha = −2,0,0.9

3.1 Euler-Maruyama Scheme

The first way I simulated the CEV process is through an Euler-Maruyama scheme over equation 5. I let the discretization be $dt = 0.001$ and the number of samples be $N = 10^6$. I also let $F_0 = 100$, $T = 4$ years, and presumed an annual lognormal volatility of $\sigma_{LN} = 0.5$. Strike prices of $K = 90, 100, 110$ and alpha values $\alpha = -2, -1, 0, 0.1, \cdots, 0.9$ were explored. On a 12th Gen Intel(R) Core(TM) i5-12600K, 3.69 GHz, with 10-core multiprocessing, simulating one set of parameters took roughly 6 minutes.

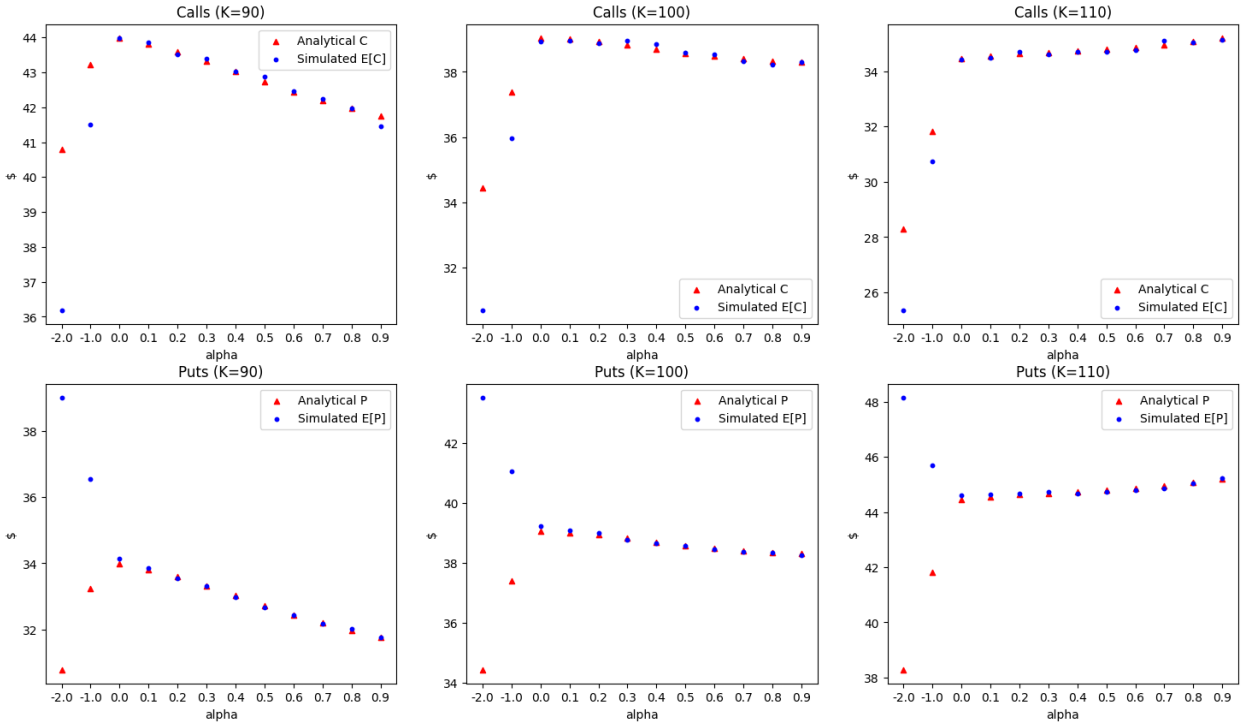

Figure 2: Comparison of Euler simulated prices to analytical options prices. Large deviations in $\alpha < 0$ are analyzed in Section 3.5

3.2 Direct Sampling

In equation 12, we defined the distribution of X as the CDF of the non-central chi-squared distribution. To find the final distribution at X_T, we sample from this CDF according to the technique defined in [7].

In principle, to sample X_T from equation 12, we let

$$U = Pr(X \leq X_T | X_0) = \chi'^2\left(\frac{X_0}{T}, 2-\delta; \frac{X_T}{T}\right), \quad F(x) = \chi'^2\left(\frac{X_0}{T}, 2-\delta; x\right), \tag{16}$$

where U is a uniformly drawn random number and compute the inverse function

$$F^{-1}(U) = \frac{X_T}{T}. \tag{17}$$

However, due to numerical challenges with accounting for absorption through this method, we account for absorption "by hand". First, we draw samples from a uniform distribution, defined as U. Then, if

$$U > U_{max} = \Gamma\left(-\nu; \frac{X_0}{2T}\right) \tag{18}$$

we set the corresponding X_T value to 0. Otherwise, we compute

$$\frac{X_T}{T} = F^{-1}(U_{max} - U) \tag{19}$$

which can be done numerically by performing a root search, finding which values of x satisfy $F(x) - U_{max} + U = 0$.

3.3 Simulations

Euler Maruyama path simulations can be found in Figure 1. Final simulated EM-scheme prices are found in Figure 2. Computed prices are from the formula found in Section 2.5. Both EM-Scheme and direct sampling values and standard error measurements can be found in tabular data forms in Appendix B. Additionally, in Section 2.4, we established that the absorption rate for simulated paths could be computed by a gamma function relationship. We verify our EM Scheme simulations with a plot of alpha versus absorption ratio in Figure 3.

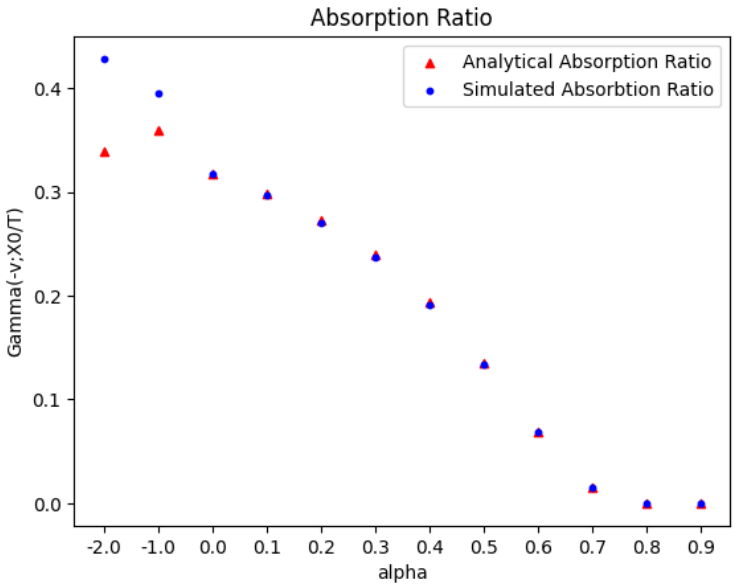

Figure 3: Evaluation of EM-scheme simulated absorption ratio against analytical absorption ratio. Again, deviations in $\alpha < 1$ cas are addressed in Section 3.5

3.4 Comparison of EM-Scheme to Direct Sampling

Overall, both EM-Scheme and direct sampling methods are rather computationally intensive. However, direct sampling holds a significant advantage over EM-Scheme in accuracy.

Since the EM-Scheme introduces discretization error, for certain values of α as presented in the next section or large values of T, the EM-Scheme simulated prices will gradually separate from the analytical prices. Accounting for discretization errors requires significant computational resources. Additionally, applying quasi-Monte Carlo sampling to discretization methods is more complex than applying to direct sampling, increasing room for error.

3.5 Discretization Error in $\alpha < 0$

In both Figures 2 and 3, it is clear that the Euler scheme is somehow failing for the $\alpha < 0$ case. However, when observing the paths in Figure 1, it is not evident where precisely the Euler simulation is going wrong. I conducted a simple discretization test to observe the rate of convergence and error measurements, changing $dt = 0.002, 0.001, 0.0005$. Results are shown in Figure 4. The reduction in error seems to appear linearly related to the $\log_2$ of dt. Extrapolating this linear relationship, it appears that dt must be shrunken roughly 9 and 45 times from $dt = 0.0005$ for accurate simulations of $\alpha = -1$ and $\alpha = -2$, respectively. However, this would be computationally intractable and consume significant amounts of memory.

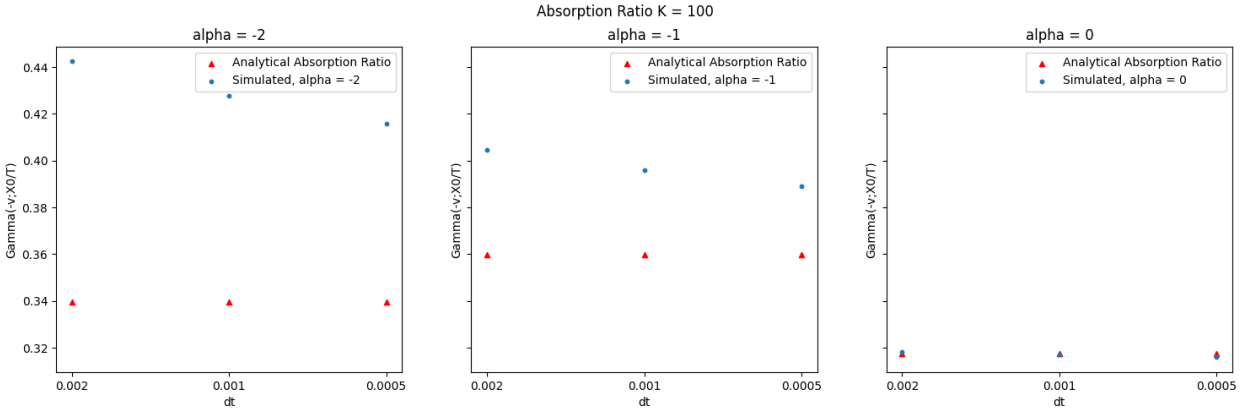

(a) Absorbtion ratio as dt is decreased

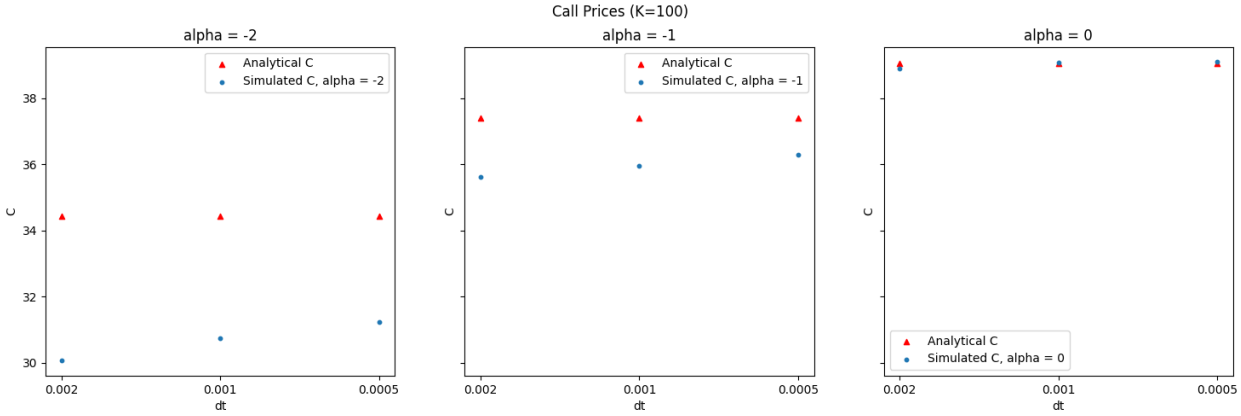

(b) Simulated C price as dt is decreased

Figure 4: An analysis of EM-scheme discretization error for $K = 100$ and $\alpha < 0$

4 Conclusions and Future Work

As an exploration of the CEV process, there is not much conclusion to be drawn. However, I found many parts interesting. It was surprising that F could be transformed into a well-known Bessel function, such that the resulting transition density function was related to the non-central chi-squared distribution. Additionally, the absorption actually follows a function. This was intriguing to confirm via path simulations. Furthermore, it was surprising that the Euler scheme would start failing drastically for certain parameter schemes despite nothing wrong with the values. Significantly smaller discretization increments are required to sample $\alpha < 0$ cases. Additionally, the computational cost of the Euler scheme makes it rather infeasible for actual application in a time-sensitive field such as finance.

Future work could explore the $\alpha > 1$ case, more mathematical derivations, or evaluate Monte Carlo Simulations using the method mentioned in [7]. A particularly interesting exploration would be taking real equity data, back-calculating α, computing expected prices, and comparing them to actual prices.

References

[1] F. Black and M. Scholes. The pricing of options and corporate liabilities. *Journal of Political Economy*, 81(3):637–654, 1973.

[2] J. C. Cox. The constant elasticity of variance option pricing model. *The Journal of Portfolio Management*, 23(5):15–17, 1996.

[3] W. Feller. Two singular diffusion problems. *The Annals of Mathematics*, 54(1):173, 1951.

[4] H. Geman and Y. F. Shih. Modeling commodity prices under the cev model. *The Journal of Alternative Investments*, 11(3):65–84, 2008.

[5] Y. Hsu, T. Lin, and C. Lee. Constant elasticity of variance (cev) option pricing model: Integration and detailed derivation. *Mathematics and Computers in Simulation*, 79(1):60–71, 2008.

[6] J. Hull. *Options, futures, and other derivatives*. Pearson Education Limited, 2022.

[7] A. Lindsay and D. Brecher. Simulation of the cev process and the local martingale property. *Mathematics and Computers in Simulation*, 82(5):868–878, 2012.

[8] M. SCHRODER. Computing the constant elasticity of variance option pricing formula. *The Journal of Finance*, 44(1):211–219, 1989.

[9] J. Yu. On leverage in a stochastic volatility model. *Journal of Econometrics*, 127(2):165–178, 2005.

A Verification of Squared Bessel Process

$$X = \frac{F^{2(1-\alpha)}}{\sigma^2(1-\alpha)^2}, \quad dX = \delta dt + \sigma\sqrt{X}dW, \quad \delta = \frac{1-2\alpha}{1-\alpha}$$

$$dF = \sigma F^{\alpha} dW = A(x)dt + B(x)dW$$

$$A(x) = 0, B(x) = \sigma F^{\alpha}, X_t = 0, X_{F(x)} = \frac{2F^{1-2\alpha}}{(1-\alpha)\sigma^2}, X_{F(x),F(x)} = \frac{(4\alpha-2)F^{-2\alpha}}{(\alpha-1)\sigma^2 k}$$

$$\begin{aligned} dX &= (X_t + X_{F(t)}A(t) + \frac{1}{2}X_{F(t),F(t)}B(t)^2)dt + (X_{F(t)}B(t))dW \\ &= (0 + 0 + \frac{1}{2}\frac{(4\alpha-2)F^{-2\alpha}}{(\alpha-1)\sigma^2}(\sigma F^{\alpha})^2)dt + (\frac{2F^{1-2\alpha}}{(1-\alpha)\sigma^2}\sigma F^{\alpha})dW \\ &= \frac{(1-2\alpha)}{(1-\alpha)}dt + 2\frac{F^{1-\alpha}}{\sigma(1-\alpha)}dW \\ &= \delta dt + 2\sqrt{X}dW \quad \delta = \frac{(1-2\alpha)}{(1-\alpha)} \end{aligned} \tag{20}$$

B Results

Table 1: Simulated Call values for $K = 90$

α	**EM Simulated Calls**	**Direct Sampling Simulated Calls**	**Analytical Calls**
-2.0	36.18731±0.03790	40.78903±0.036370	40.78008
-1.0	41.51010±0.04638	43.26115±0.04512	43.22324
0.0	43.96978±0.06202	44.31783±0.06028	43.98810
0.1	43.86517±0.06429	44.24568±0.06252	43.81491
0.2	43.52320±0.06678	44.15167±0.06499	43.58715
0.3	43.39890±0.06984	44.05041±0.06775	43.31587
0.4	43.01630±0.07303	43.95269±0.07090	43.02013
0.5	42.86400±0.07700	43.83011±0.07457	42.72311
0.6	42.45335±0.08145	43.52073±0.07901	42.44314
0.7	42.23271±0.08694	42.52495±0.08473	42.18755
0.8	41.97058±0.09372	41.95676±0.09161	41.95654
0.9	41.46066±0.10218	41.74849±0.10067	41.74881

Table 2: Simulated Put values for $K = 90$

α	**EM Simulated Puts**	**Direct Sampling Simulated Puts**	**Analytical Puts**
-2.0	39.01907±0.04450	30.78888±0.03636	30.78008
-1.0	36.54361±0.04374	33.26114±0.04512	33.22324
0.0	34.13850±0.04090	34.31734±0.06028	33.98810
0.1	33.86517±0.04021	34.24565±0.06252	33.81491
0.2	33.54140±0.03935	34.15104±0.06499	33.58715
0.3	33.30209±0.03837	34.05036±0.06775	33.31587
0.4	32.97611±0.03721	33.95266±0.07090	33.02013
0.5	32.67832±0.03588	33.83016±0.07457	32.72311
0.6	32.43711±0.03451	33.52075±0.07901	32.44314
0.7	32.17374±0.03313	32.52414±0.08471	32.18755
0.8	32.01302±0.03183	31.95659±0.09160	31.95654
0.9	31.75865±0.03059	31.74844±0.10067	31.74881

Table 3: Simulated Call values for $K = 100$

α	**EM Simulated Calls**	**Direct Sampling Simulated Calls**	**Analytical Calls**
-2.0	30.68502±0.03374	34.42930±0.03258	34.42928
-1.0	35.95739±0.04249	37.38738±0.04146	37.38750
0.0	38.92345±0.05834	39.04476±0.05709	39.04516
0.1	38.95621±0.06084	39.00884±0.05942	39.00887
0.2	38.87104±0.06345	38.93075±0.06201	38.93070
0.3	38.95016±0.06670	38.82067±0.06491	38.82097
0.4	38.85327±0.07012	38.69682±0.06822	38.69619
0.5	38.58408±0.07369	38.57566±0.07203	38.57528
0.6	38.54010±0.07852	38.47175±0.07652	38.47236
0.7	38.31322±0.08392	38.39305±0.08200	38.39279
0.8	38.21156±0.09111	38.33720±0.08891	38.33676
0.9	38.30854±0.10052	38.30349±0.09817	38.30351

Table 4: Simulated Put values for $K = 100$

α	**EM Simulated Puts**	**Direct Sampling Simulated Puts**	**Analytical Puts**
-2.0	43.53105±0.04934	34.42930±0.03258	34.42928
-1.0	41.05997±0.04841	37.38738±0.04146	37.38750
0.0	39.21799±0.04509	39.04476±0.05709	39.04516
0.1	39.09999±0.04434	39.00884±0.05942	39.00887
0.2	38.98962±0.04346	38.93075±0.06201	38.93070
0.3	38.76909±0.04238	38.82067±0.06491	38.82097
0.4	38.66758±0.04116	38.69682±0.06822	38.69619
0.5	38.57982±0.03979	38.57566±0.07203	38.57528
0.6	38.46275±0.03836	38.47175±0.07652	38.47236
0.7	38.37608±0.03694	38.39305±0.08200	38.39279
0.8	38.33880±0.03558	38.33720±0.08891	38.33676
0.9	38.25522±0.03429	38.30349±0.09817	38.30351

Table 5: Simulated Call values for $K = 110$

α	**EM Simulated Calls**	**Direct Sampling Simulated Calls**	**Analytical Calls**
-2.0	25.35551±0.02964	28.28016±0.02884	28.28014
-1.0	30.73917±0.03872	31.81076±0.03778	31.81087
0.0	34.41975±0.05496	34.44677±0.05367	34.44670
0.1	34.49657±0.05737	34.55385±0.05606	34.55387
0.2	34.70268±0.06019	34.63007±0.05870	34.63001
0.3	34.60384±0.06297	34.68406±0.06167	34.68438
0.4	34.69962±0.06651	34.73072±0.06505	34.73094
0.5	34.70750±0.07037	34.78534±0.06895	34.78498
0.6	34.77222±0.07520	34.85689±0.07355	34.85746
0.7	35.09838±0.08136	34.95272±0.07916	34.95247
0.8	35.05481±0.08821	35.07100±0.08623	35.07041
0.9	35.15077±0.09764	35.21184±0.09570	35.21113

Table 6: Simulated Put values for $K = 100$

α	**EM Simulated Puts**	**Direct Sampling Simulated Puts**	**Analytical Puts**
-2.0	48.16271±0.05409	38.28016±0.02884	38.28014
-1.0	45.69526±0.05293	41.81076±0.03778	41.81087
0.0	44.60033±0.04917	44.44677±0.05367	44.44670
0.1	44.63636±0.04836	44.55385±0.05606	44.55387
0.2	44.65760±0.04742	44.63007±0.05870	44.63001
0.3	44.72490±0.04627	44.68406±0.06167	44.68438
0.4	44.66912±0.04499	44.73072±0.06505	44.73094
0.5	44.74605±0.04357	44.78534±0.06895	44.78498
0.6	44.78326±0.04209	44.85689±0.07355	44.85746
0.7	44.87004±0.04061	44.95272±0.07916	44.95247
0.8	45.05617±0.03923	45.07100±0.08623	45.07041
0.9	45.22257±0.03786	45.21184±0.09570	45.21113